

Mass dependence of the hairpin vertex in quenched QCD

Stephen R. Sharpe*

Physics Department, University of Washington, Seattle, WA 98195-1560

The pseudoscalar “hairpin” vertex (i.e. quark-disconnected vertex) plays a key role in quenched chiral perturbation theory. Direct calculations using lattice simulations find that it has a significant dependence on quark mass. I show that this mass dependence can be used to determine the quenched Gasser-Leutwyler constant L_5 . This complements the calculation of L_5 using the mass dependence of the axial decay constant of the pion. In an appendix, I discuss power counting for quenched chiral perturbation theory and describe the particular scheme used in this paper.

I. INTRODUCTION

Although the quenched approximation to QCD is being gradually superseded by unquenched simulations, it remains useful as a qualitative guide to the physics of QCD, and as a testing ground for new methods of discretizing light fermions. In the latter role, the unphysical chiral singularities of quenched QCD turn out to be helpful—reproducing them provides evidence that the light fermion method under study can approach the chiral limit. Examples of these singularities are the enhanced chiral logarithms in the pion mass and the pseudoscalar decay constant [1, 2]. The source of these singularities is the hairpin vertex, i.e. the appearance of a double-pole contribution in the flavor-singlet pion two-point function. In infinite volume (where the contributions of exact zero modes vanish) this vertex is the key unphysical feature of quenched QCD.

Quenched chiral perturbation theory (Q χ PT) allows one to systematically predict the form of these singularities. Although Q χ PT does not have the same theoretical underpinnings as chiral perturbation theory for unquenched QCD, and thus must be treated as a phenomenological theory, it has been quite successful in describing the properties of light pseudo-Goldstone bosons. A particularly thorough study has been undertaken by Bardeen *et al.* [3, 4] (referred to as BDET in the following).¹ They find that consistent values of the hairpin vertex can be obtained both from a direct calculation of the hairpin correlator and from fitting to the chiral logarithms predicted from loop contributions to various quantities.

There is, however, a puzzling aspect to the results for the hairpin vertex. On the one hand, the vertex is found to have substantial dependence on quark mass. As I argued in Ref. [11], this can be explained by a non-zero value for the momentum-dependent part of the hairpin ($\alpha_\Phi \sim 0.5$ in the notation explained below). On the other hand, BDET note that, at tree-level, one can also determine α_Φ from the coefficient of the sub-leading single-pole contribution to the hairpin correlator. They find that α_Φ determined in this way is much smaller than that determined from the mass dependence, and, in fact, is consistent with zero.

The purpose of this note is to resolve the discrepancy between these two methods for determining α_Φ . It turns out that, at next-to-leading-order (NLO) in quenched chiral perturbation theory, the hairpin vertex picks up a mass dependence proportional to L_5 (the quenched analog of corresponding Gasser-Leutwyler constant), in addition to that proportional to α_Φ . The coefficient of the single pole, however, is not affected at this order, and remains proportional to α_Φ alone. This allows a consistent description of the hairpin results: one should use the BDET method to determine α_Φ , with a result close to zero, while the mass dependence of the hairpin vertex determines L_5 . This provides a check of determinations of L_5 based on the mass dependence of the axial decay constant.

II. DETAILS OF CALCULATION

I consider quenched QCD with N_V valence quarks. For the following considerations I need $N_V \geq 2$, and for definiteness I use $N_V = 3$. I take all the quarks to be degenerate, since this is what has been done in numerical evaluations of the hairpin vertex. The leading order quenched chiral Lagrangian is then [1, 2]

$$\mathcal{L}_0 = \frac{f^2}{4} \text{Str} (\partial_\mu U \partial_\mu U^\dagger - \chi U - U^\dagger \chi) + m_0^2 \Phi_0^2 + \alpha_\Phi (\partial_\mu \Phi_0)^2, \quad (1)$$

*Electronic address: sharpe@phys.washington.edu

¹ See also the work of Refs. [5, 6, 7, 8, 9, 10].

where “Str” indicates supertrace, $U = \exp(2i\Phi/f)$ is an element of $U(3|3)$, Φ contains the pseudo-Goldstone bosons and fermions, and $\Phi_0 = \text{Str}(\Phi)/\sqrt{3}$ is the “super- η' ” field. Quark masses are contained within $\chi = 2B_0M$, where $M = \text{diag}(m, m, m, m, m, m)$ is the mass matrix of quarks and ghost-quarks. I assume that m is small enough that it is appropriate to use chiral perturbation theory to describe the properties of the pseudo-Goldstone hadrons.

The parameters f (pion axial decay constant in the chiral limit, normalized so it is close to 90 MeV) and B_0 are the quenched analogs of the corresponding parameters that appear in the unquenched chiral Lagrangian. The parameters m_0 and α_Φ are, however, special to quenched chiral perturbation theory, in which one cannot integrate out the Φ_0 . In the large N_c and chiral limits, one can show that $m_0 = m_{\eta'}$ [1, 2]. Assuming this holds also at $N_c = 3$, one expects $m_0 \approx 0.85$ GeV. The presence of the new mass-scale m_0 gives rise to the enhanced singularities of the quenched theory, the strength of which is parameterized by $\delta = m_0^2/(48\pi^2 f^2)$. It will be useful in the following to keep in mind the approximate value of δ . The naive estimate (using QCD values for the parameters) is $\delta \approx 0.2$, while simulations find values in the range $\delta = 0.1 - 0.2$ (for a recent review see Ref. [12]). What is most important about these values is that they are small.

The present calculation will be performed at NLO in a power counting scheme for quenched chiral perturbation theory described in the appendix. It will require the standard NLO Lagrangian of the unquenched theory, suitably generalized by changing traces to supertraces, plus an additional term:

$$\begin{aligned} \mathcal{L}_{1A} = & -L_1 [\text{Str}(\partial_\mu U \partial_\mu U^\dagger)]^2 - L_2 \text{Str}(\partial_\mu U \partial_\nu U^\dagger) \text{Str}(\partial_\mu U \partial_\nu U^\dagger) - L_3 \text{Str}(\partial_\mu U \partial_\mu U^\dagger \partial_\nu U \partial_\nu U^\dagger) \\ & + L_4 \text{Str}(\partial U \partial U^\dagger) \text{Str}(\chi U^\dagger + U \chi) + L_5 \text{Str}(\partial U \partial U^\dagger [\chi U^\dagger + U \chi]) - L_6 [\text{Str}(\chi U^\dagger + U \chi)]^2 \\ & - L_7 [\text{Str}(\chi U^\dagger - U \chi)]^2 - L_8 \{ \text{Str}(U \chi U \chi) + \text{Str}(\chi U^\dagger \chi U^\dagger) \} \\ & - L_Q \text{Str}(\partial_\mu U \partial_\nu U^\dagger \partial_\mu U \partial_\nu U^\dagger). \end{aligned} \quad (2)$$

Here L_{1-8} are the quenched analogs of the corresponding Gasser-Leutwyler coefficients. L_Q multiplies an operator which is not independent in unquenched $SU(2)$ or $SU(3)$ chiral perturbation theory, but which is independent in the quenched and partially quenched theories. Its presence in partially quenched theories was noted and explained recently [13]. That it is also needed in the quenched theory can be seen by generalizing the arguments given there.

In the quenched theory, one must also include other operators obtained from those in \mathcal{L}_0 and \mathcal{L}_{1A} by multiplying by powers of Φ_0 . These introduce many new constants. It turns out, however, that the resulting operators do not contribute at NLO to the quantities I consider here, as explained in the appendix. For illustration, I list two of the leading operators of this type:

$$\mathcal{L}_{1B} = v_0(m_0^2/f^2)\Phi_0^4 - v_8 L_8(i\Phi_0/f) \{ \text{Str}(U \chi U \chi) - \text{Str}(\chi U^\dagger \chi U^\dagger) \}, \quad (3)$$

where $v_{0,8}$ are additional couplings.

Following BDET, I consider the following correlation functions:

$$\tilde{\Delta}_c(p) = \int_x e^{-ip \cdot x} \langle \bar{q}_A \gamma_5 q_B(x) \bar{q}_B \gamma_5 q_A(0) \rangle, \quad (4)$$

$$\tilde{\Delta}_h(p) = \int_x e^{-ip \cdot x} \langle \bar{q}_A \gamma_5 q_A(x) \bar{q}_B \gamma_5 q_B(0) \rangle. \quad (5)$$

Here q_A and q_B are two different valence quarks, and the expectation value indicates the quenched average. The subscripts c and h are a reminder that only quark-connected contractions contribute to $\tilde{\Delta}_c$, whereas $\tilde{\Delta}_h$ contains only quark-disconnected contractions. In other words, $\tilde{\Delta}_c$ is the usual non-singlet pseudoscalar two-point correlator, while $\tilde{\Delta}_h$ is the pseudoscalar hairpin correlator. These are the correlators used in simulations to study the hairpin vertex.

At low momenta the connected correlator is well described by a single pole

$$\tilde{\Delta}_c(p) = -\frac{f_P^2}{p^2 + M_\pi^2} + \text{non-pole}, \quad (6)$$

where f_P is, by definition, the pseudoscalar decay constant, and the sign arises from Wick contractions. By contrast, the hairpin correlator is observed to have a leading double-pole contribution:

$$\tilde{\Delta}_h(p) = \mathcal{D} \frac{f_P^2}{(p^2 + M_\pi^2)^2} + \mathcal{S} \frac{f_P^2}{p^2 + M_\pi^2} + \text{non-pole}, \quad (7)$$

where f_P is to be determined from eq. (6). I will refer to the residues \mathcal{D} and \mathcal{S} as the hairpin and single-pole coefficients, respectively. They are defined to be independent of p^2 , but can depend on m_q , as do f_P and M_π .

With this notation in hand, I can now state more precisely the observations made in BDET and previous work. These are, first, that $\mathcal{S} \approx 0$, i.e. that $\tilde{\Delta}_h(p)$ is consistent with a pure double-pole; and, second, that \mathcal{D} has a significant mass dependence. I now turn to the predictions of the quenched chiral Lagrangian for \mathcal{D} and \mathcal{S} .

To begin with I need to determine the operator in the effective theory which matches onto the pseudoscalar density. This can be done, as in unquenched chiral perturbation theory, by taking appropriate derivatives with respect to the quark mass matrix, treating the latter as a source. At leading order, using \mathcal{L}_0 , this gives $\bar{q}_A \gamma_5 q_B \rightarrow 2iB_0 f \Phi_{AB} + O(\Phi^3)$, for all A and B , leading to the tree-level results

$$\tilde{\Delta}_c(p) = -\frac{(2B_0 f)^2}{p^2 + \chi} \quad (8)$$

$$\tilde{\Delta}_h(p) = \frac{(m_0^2 + \alpha_\Phi p^2)}{3} \frac{(2B_0 f)^2}{(p^2 + \chi)^2}. \quad (9)$$

Comparing to eqs. (6) and (7) I find

$$M_\pi^2 = \chi; \quad f_P = 2B_0 f; \quad \mathcal{D} = \frac{m_0^2 - \alpha_\Phi M_\pi^2}{3}; \quad \mathcal{S} = \frac{\alpha_\Phi}{3}. \quad (10)$$

These leading order results are well known [1], and agree with those quoted in BDET when normalization and sign conventions are taken into account.

As noted above, at this order α_Φ provides both the mass dependence of \mathcal{D} and the value for \mathcal{S} . It is perhaps worth understanding this point in more detail. One might have thought that a term in \mathcal{L}_0 of the form

$$(f^2/4)v_2 \text{Str}(\chi U^\dagger - U\chi) i\Phi_0/f \quad (11)$$

would provide additional mass dependence to the hairpin vertex, and thus break the correlation between \mathcal{D} and \mathcal{S} . However, this term also contributes to the effective field theory expression for the pseudoscalar density, and leads to an additional term in \mathcal{S} , in such a way that v_2 can be absorbed into a redefinition of α_Φ . This is a consequence of the fact, noted in Ref. [1], that the v_2 term (11) can be removed by a field redefinition [explicitly this is $U \rightarrow U \exp(-iv_2 \Phi_0/f)$] and a redefinition of parameters ($\alpha_\Phi \rightarrow \alpha_\Phi - \sqrt{3}v_2$).

Before proceeding to the details of the NLO calculation, it is necessary to discuss the power counting appropriate to quenched chiral perturbation theory. I give an overview here and a comprehensive discussion in the appendix. Standard unquenched chiral perturbation theory is, in the meson sector, an expansion in $\epsilon^2 \sim M_\pi^2/\Lambda_\chi^2 \sim p^2/\Lambda_\chi^2$, where $\Lambda_\chi = 4\pi f$. The issue in quenched chiral perturbation theory is how to treat the extra constants that appear, the most important of which is m_0 . This appears in two dimensionless combinations in the calculations considered here. First, loop contributions are suppressed by powers of $\delta = m_0^2/(3\Lambda_\chi^2)$, which, as noted above, is numerically small.² Second, the ratio of the two terms contributing to \mathcal{D} in eq. (10) is $\alpha_\Phi M_\pi^2/m_0^2$. It is also reasonable to treat this combination as small, given that m_0 is close to Λ_χ and α_Φ is small. To do so consistently, however, one must develop a systematic power counting scheme in which both combinations are small, and for which one can assess the relative size of other contributions.

Two such schemes are explained in the appendix. In the first (the standard or **PC1** scheme) one takes $\delta \sim \alpha_\Phi/3 \sim \epsilon^2$, while in the second (the **PC2** scheme) $\delta \sim \alpha_\Phi/3 \sim \epsilon^{4/3}$. In both schemes the α_Φ contribution to \mathcal{D} is non-leading:

$$\frac{\alpha_\Phi M_\pi^2}{m_0^2} = \frac{\alpha_\Phi}{3} \frac{\epsilon^2}{\delta} \sim \epsilon^2 \quad \textbf{PC1/PC2}. \quad (12)$$

The schemes differ, however, in the size of other contributions. In the **PC2** scheme, since δ is larger than ϵ^2 , “second-order” terms of size δ^2 , $\delta\epsilon^2$, and ϵ^4 are progressively smaller, while all three are treated as of the same size in **PC1**. Thus the **PC2** scheme has some similarities to that used in BDET, in which terms of relative size $\delta\epsilon^2 \log(M_\pi/\mu)$ are kept, but those of size ϵ^4 are not. This point is discussed further in the appendix.

² In fact, the leading logarithmic corrections are proportional to powers of $\delta \log(M_\pi/\mu)$, with μ the regularization scale, and thus dominate over the leading term in the extreme chiral limit. For most practical simulations, however, including those of BDET, the logarithm is of $O(1)$, and does not lead to a significant enhancement. I assume this to be case in the power counting schemes I use.

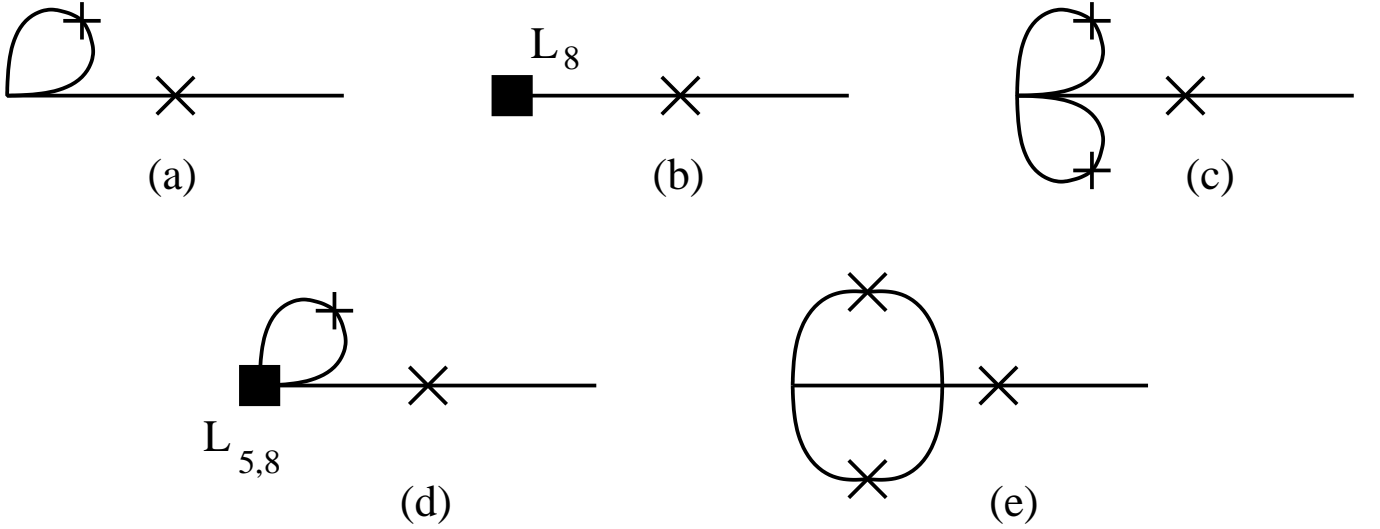


FIG. 1: Examples of diagrams contributing to the pseudoscalar hairpin correlator which are associated with vertex renormalization. Simple vertices are from the first two terms in \mathcal{L}_0 , crosses indicate m_0 or α_Φ vertices, filled boxes are interactions from \mathcal{L}_{1A} , with the specific term which contributes being noted. Note that if the rightmost propagator and hairpin vertex are removed, these become contributions to the quark-connected correlator.

In this paper I calculate the connected and disconnected correlators at NLO in the **PC2** scheme. By NLO I mean that corrections of size up to and including ϵ^2 relative to the leading contribution are included. After amputation, the disconnected vertex has the form $\mathcal{D} + (p^2 + M_\pi^2)\mathcal{S} + \dots$, from which one can extract \mathcal{D} and \mathcal{S} . Note that one obtains a lower order result for \mathcal{S} than for \mathcal{D} because of the explicit factor of $(p^2 + M_\pi^2)$ multiplying \mathcal{S} .

I choose the **PC2** scheme because it reduces the number of diagrams that contribute and thus simplifies the calculation. In both schemes, however, the general point is the same: there are other terms which contribute at the same order as the α_Φ vertex, and these must be included.

The calculation of the connected correlator is standard and leads to the replacement of f_P and M_π^2 in eq. (6) with their NLO expressions. The leading diagrams that contribute can be deduced from those in figs. 1 and 3 by removing the rightmost propagator and the hairpin vertex to which it couples. As can be seen from table I, a NLO calculation involves only diagrams (a) and (b) from both figures—other diagrams are of higher order than ϵ^2 in both power counting schemes. The explicit expressions for f_P and M_π^2 are given in BDET and elsewhere, with the latter repeated in the Appendix, eq. (A8). They are not needed to determine \mathcal{D} and \mathcal{S} .

For the disconnected correlator, one can divide the contributions into the four classes. (1) Those renormalizing the external pseudoscalar density, and which would be present also if the density were flavor non-singlet. Examples of these are shown in fig. 1. (2) Those renormalizing the external density, but which are present only because the density is flavor singlet. These contribute only to the single pole amplitude \mathcal{S} , but not to \mathcal{D} . Examples are shown in fig. 2. (3) Those renormalizing the mass and wavefunction of the pseudo-Goldstone boson, shown in fig. 3. (4) Those associated with the hairpin vertex, shown in fig. 4. Two observations greatly simplify the calculation. First, the contributions of classes (1) and (3) are identical to those appearing in the connected correlator. This means that the same expressions for f_P and M_π^2 apply to both connected and disconnected correlators—as one would have expected. Second, all contributions of classes (2) and (4), aside from the leading order diagram fig. 4(a), are smaller than NLO.³

These observations imply that the sole NLO correction to the hairpin vertex in the **PC2** scheme comes from wavefunction renormalization. This in turn arises at NLO only from fig. 3(b), as fig. 3(a) only renormalizes the mass. Since there are two boson propagators in the disconnected correlator, compared to only one in the connected correlator, only “half” of the wavefunction renormalization in the disconnected case is absorbed into the one-loop

³ This simplification does not occur in the **PC1** scheme, in which at NLO one must also calculate figs. 2(a-b) and 4(b-c).

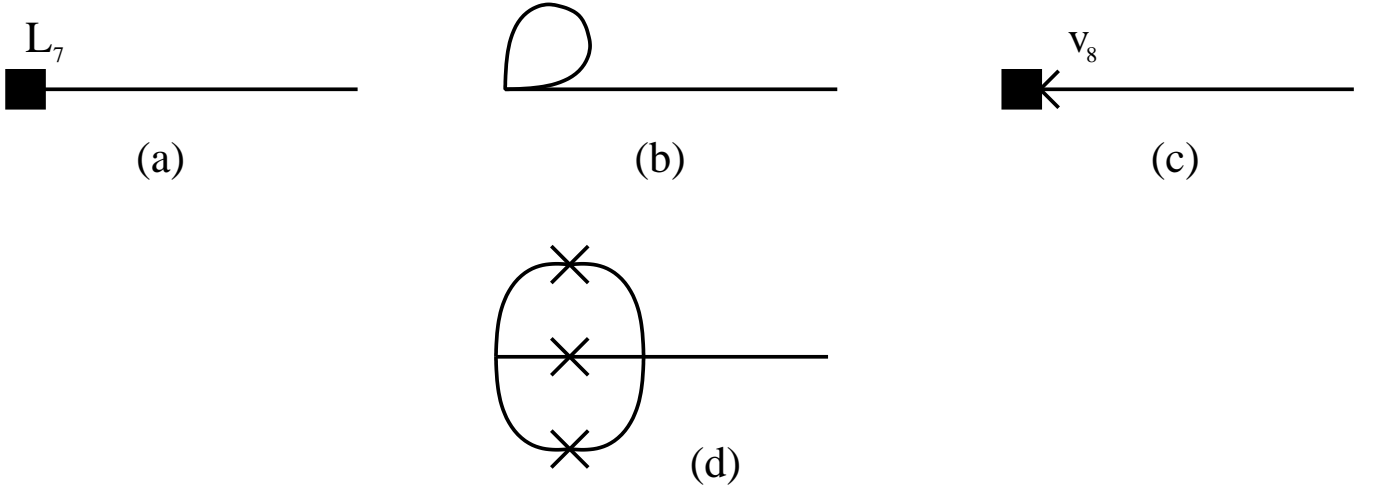


FIG. 2: Examples of diagrams contributing to the pseudoscalar hairpin correlator which contribute directly to the single pole residue \mathcal{S} . Notation is as in figs. 1, except that boxes with attached arrowheads are from \mathcal{L}_{1B} (the arrowhead indicating the Φ_0 field).

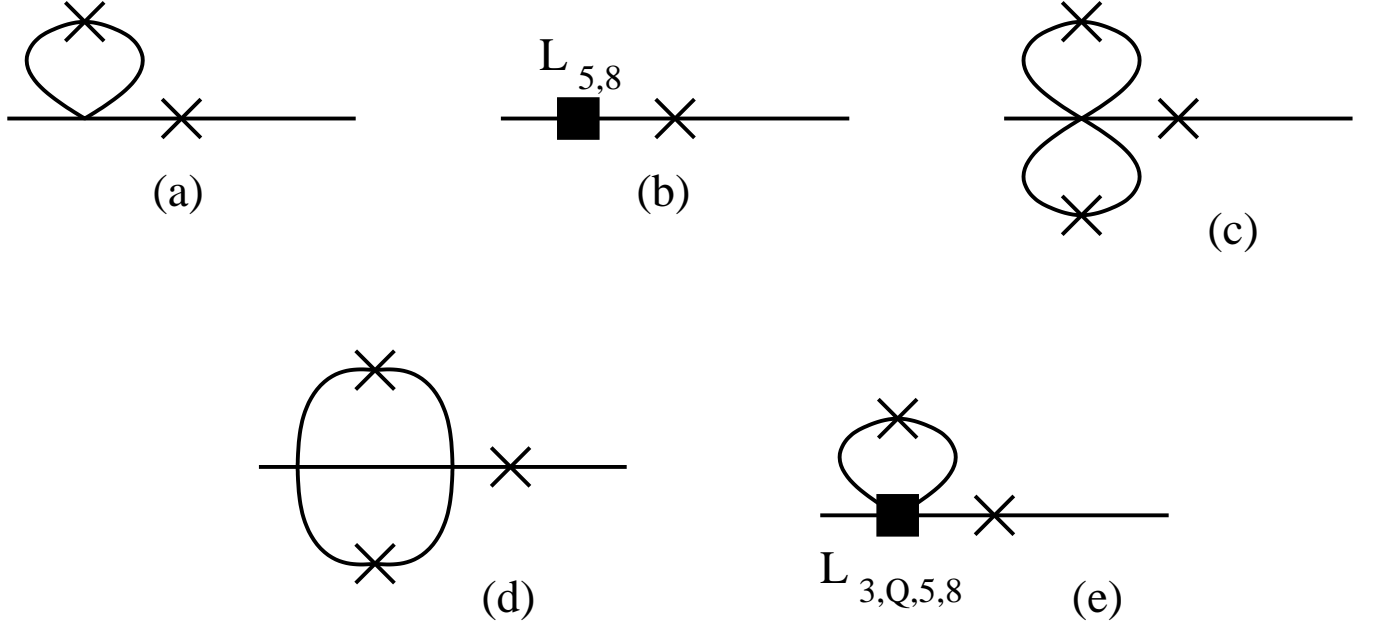


FIG. 3: Examples of diagrams contributing to the pseudoscalar hairpin correlator which are associated with pion mass and wavefunction renormalization. Notation is as in fig. 1. Note that if the rightmost propagator and hairpin vertex are removed, these are contributions to the quark-connected correlator.

result for f_P^2 . The other half renormalizes the hairpin vertex, leading to the results⁴

$$\mathcal{D} = \frac{1}{3} \left\{ m_0^2 \left(1 - 8L_5 \frac{\chi}{f^2} \right) - \alpha_\Phi M_\pi^2 \right\}; \quad \mathcal{S} = \frac{\alpha_\Phi}{3}. \quad (13)$$

⁴ In an earlier version of this paper I also kept corrections of relative size $\epsilon \delta^2 \log(M_\pi/\mu)$, coming from fig. 3(e), as in the calculation of BDET. The analysis in the appendix shows that in either power counting scheme one should then also include all the other diagrams in figs. 3 and 4, including non-trivial two loop diagrams. I have not attempted this calculation.

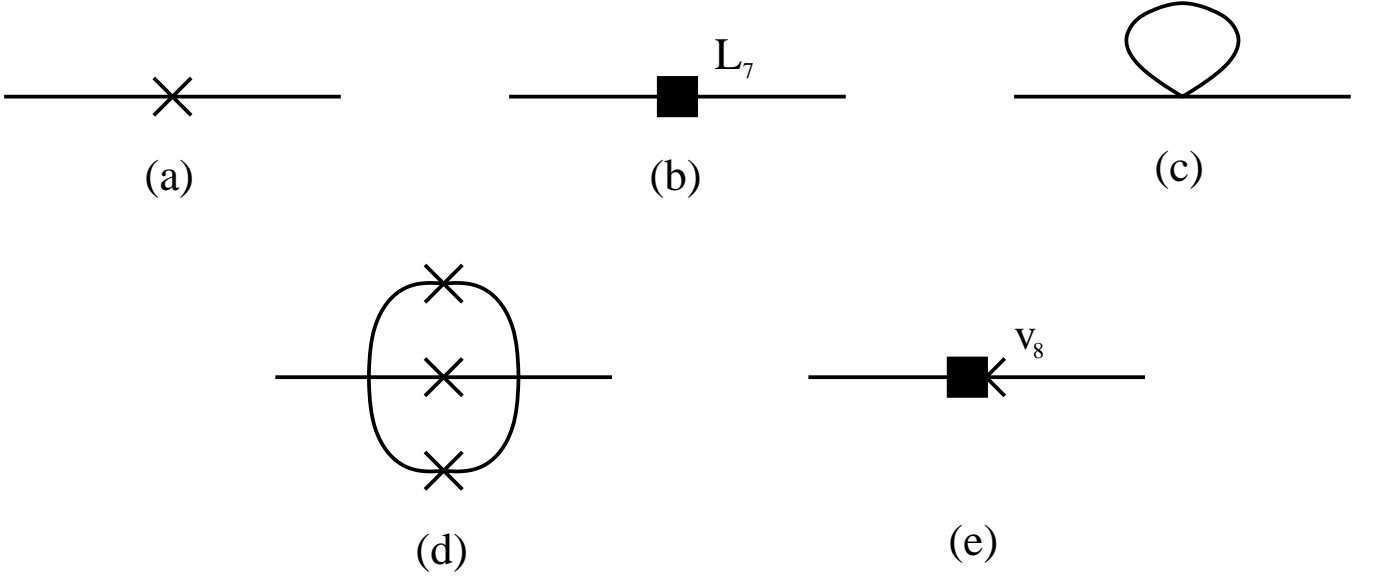


FIG. 4: Examples of diagrams contributing to the pseudoscalar hairpin correlator which are associated with renormalization of the hairpin vertex itself. Notation is as in figs. 1 and 2.

Note that the NLO contributions do not change \mathcal{S} from its tree level value in eq. (10). In particular, the correction to \mathcal{S} from wavefunction renormalization is a correction of relative size ϵ^4 in the amputated disconnected correlator, and thus beyond the order I am considering. Note also that one can interchange χ and M_π^2 in the result, as the difference is of higher order than I consider.

Equation (13) is the new result of this paper. It shows that the mass dependence of the hairpin \mathcal{D} is *not* tied to the coefficient of the single pole \mathcal{S} . Thus, in particular, the single-pole term can be absent (as found, to good approximation, by BDET), but the hairpin vertex can have a linear dependence on M_π^2 . Furthermore, the latter dependence provides an alternative method for determining L_5 .

There is a nice consistency check on the result (13). At $p = 0$, the hairpin correlator is proportional to the topological susceptibility of the pure gauge theory [15]

$$m^2 \tilde{\Delta}_h(p=0) = \chi_t = \langle \nu^2 \rangle / V, \quad (14)$$

where m is the quark mass, ν the topological charge, and V the four dimensional volume. This is the “fermionic” method for measuring the susceptibility. Since this formula holds for any m , and χ_t , being a pure gauge quantity, is independent of m , the left-hand-side should also be independent of m . Inserting eq. (13) into the general form (7) I find

$$m^2 \tilde{\Delta}_h(p=0) = \frac{m^2 f_P^2}{M_\pi^4} (\mathcal{D} + \mathcal{S} M_\pi^2 + O(M_\pi^4)) \quad (15)$$

$$= \frac{m^2 f_P^2 m_0^2}{3 M_\pi^4} \left(1 - 8 L_5 \frac{\chi}{f^2} \right) \quad (16)$$

$$= \frac{f_A^2 m_0^2}{12} \left(1 - 8 L_5 \frac{\chi}{f^2} \right). \quad (17)$$

where in the last step I have used the axial Ward identity $2m f_P = M_\pi^2 f_A$, which holds to all orders in chiral perturbation theory (and can be checked at NLO from the expressions in BDET).⁵ Using the expression given in BDET for the axial decay constant f_A , I find

$$m^2 \tilde{\Delta}_h(p=0) = \frac{f^2 m_0^2}{6}. \quad (18)$$

⁵ Here I use the BDET normalization such that $f_A = \sqrt{2}f$ in the chiral limit.

This is independent of the quark mass, as required.

One can try turning this argument around, i.e. assuming (18) and deriving eq. (13). This will, however, only constrain the combination $\mathcal{D} + M_\pi^2 \mathcal{S}$, and not allow a separate determination of \mathcal{D} and \mathcal{S} .

I close this section with a technical comment. In order to predict the coefficient of the single pole in the hairpin correlator one must control the corrections to the operator which creates the meson at $O(p^2)$ relative to the leading order. This is because such a correction multiplying the double-pole leads to a contribution to the single-pole. Thus it is crucial that one calculate the hairpin correlator with an operator which can be matched onto the effective theory without introducing additional coefficients at $O(p^2)$. This is only true for the pseudoscalar density, used here, and for the axial current. With any other operator coupling to the pseudoscalar meson, e.g. $\bar{q}\partial^2\gamma_5 q$, the coefficient of the single pole could not be predicted.

In light of this discussion, one might be concerned about the need to include the operator

$$\text{Str}(\chi\partial^2[U + U^\dagger]) \quad (19)$$

in \mathcal{L}_{1A} , since this would give a contribution to the pseudoscalar density proportional to $p^2\Phi$. It turns out, however, that this operator can be removed (as in unquenched chiral perturbation theory) by a field definition and appropriate shifts in L_5 , L_8 and α_Φ . Thus it is a redundant operator.⁶ I have checked this by explicitly calculating its contributions to f_A , f_P and $\tilde{\Delta}_{c,h}$.

III. CONCLUSION

In this note I have presented a complete NLO calculation of the hairpin vertex in quenched chiral perturbation theory. The result, eq. (13), resolves a puzzle concerning the determination of the parameter α_Φ . The method I had proposed in Ref. [11], using the quark mass dependence of the residue of the double-pole, turns out to be incorrect. The correct method is to use the residue of the single-pole, which, according to BDET, leads to $0 \approx \alpha_\Phi \ll 1$. The mass dependence of the double-pole residue then allows one to determine L_5 .

It will be interesting to reanalyze the results of BDET and earlier work in this light, and compare the determinations of L_5 with those obtained from the mass dependence of the axial decay constant, f_A . As a rough first attempt, I note that my earlier estimate $\alpha_\Phi \approx 0.5$ converts to $L_5 \approx 0.5/(48\pi^2\delta) \approx 1.3 \times 10^{-3}$, where I have taken $\delta = 0.1$ from BDET for the value of the hairpin vertex in the chiral limit. This is close to the values for L_5 quoted in BDET.

The calculation also suggests a simple way of displaying the consistency of the different determinations of the parameters of quenched chiral perturbation theory. It follows from the previous considerations that

$$(\mathcal{D} + M_\pi^2 \mathcal{S})f_A^2 = 4\chi_t + O(M_\pi^4). \quad (20)$$

In the notation of BDET, this means that the combination $[(m_0^{\text{eff}})^2 + M_\pi^2 \alpha_\Phi] \times f_A^2$ should be independent of m at linear order. Since α_Φ is small, this constraint explains the observed result that m_0^{eff} decreases with increasing m in terms of the fact that f_A increases with m .

When applying the results of this paper to numerical simulations, one should keep in mind that the previous discussion did not account for finite volume or discretization errors. Concerning the former, one can include the leading effect by replacing the loop integrals with those appropriate to finite volume. As for the discretization errors, if one uses Wilson-like fermions, then there will be $O(am)$ corrections to the results presented here, unless the action and operators are non-perturbatively $O(a)$ improved (which is not the case in the work of BDET). This is because of the breaking of chiral symmetry by the action. In particular, the quantity in eq. (20) will have a mass dependence proportional to am . Thus a possible use of this relation is to gauge the size of such discretization errors.

Acknowledgments

I thank Martin Savage and Ruth Van de Water for comments on the manuscript, and Bill Bardeen and Maarten Golterman for discussions. This work was supported in part by the US Department of Energy through grant DE-FG03-96ER40956/A006.

⁶ I am grateful to Bill Bardeen for helpful discussions on this point.

APPENDIX A: POWER COUNTING IN QUENCHED CHIRAL PERTURBATION THEORY

In this appendix I discuss power counting schemes for quenched chiral perturbation theory, and explain that used for the calculation described in the main text. I also take the opportunity to collect some results that are presumably known to workers in the field but which, as far as I know, are not available in the literature. I use the standard notation for the chiral power counting parameter: $\epsilon^2 = \chi/\Lambda_\chi^2$, where χ refers to either M_π^2 or p^2 .

To make the arguments I will frequently use the fact that, in the quenched theory, diagrams involving pions (and their graded partners) can be converted in a precise, well-defined way, into those involving quark (and ghost quark) lines. This involves following flavor indices, and is allowed because of the necessary inclusion of the Φ_0 field in quenched chiral perturbation theory [1, 17]. The advantage of the quark-line representation is that the impact of quenching is transparent: all diagrams with internal quark lines cancel against those with corresponding ghost quark lines. In the following I only consider the diagrams which remain after such cancellations have occurred, i.e. I consider power counting only for diagrams that give non-trivial contributions.

1. Power counting with \mathcal{L}_0

The largest contributions to correlators involve vertices from \mathcal{L}_0 , eq. (1), so I consider first the power counting appropriate for this Lagrangian alone. For diagrams with no m_0^2 and α_Φ vertices, standard chiral power counting gives the following result for the amputated N-point correlation function with external momenta of $O(M_\pi^2)$:⁷

$$\mathcal{A}_N \sim \frac{\chi}{f^{N-2}} (\epsilon^2)^{n_\ell}, \quad n_\ell = \text{number of loops}. \quad (\text{A1})$$

For example, at leading order the two-point correlator gives the pion mass, $\mathcal{A}_2 \sim \chi \sim M_\pi^2$, with corrections suppressed by the number of loops.

This result, and those that follow, also apply to the N-point correlator of the pseudoscalar density, except that eq. (A1) must be multiplied by f^N . Since what matters is the relative size of different terms, and not the overall factor, the ensuing analysis will be directly applicable to the correlators considered in the main text.

Including m_0^2 and α_Φ vertices, I note that each such vertex introduces an extra propagator compared to the diagram without the vertex, and so their contributions (after subtracting divergences so that loop momenta are of order M_π^2) are

$$m_0^2 \text{ vertex} \sim \frac{m_0^2/3}{p^2 + M_\pi^2} \sim \frac{m_0^2}{3\chi} = \frac{\delta}{\epsilon^2}, \quad \alpha_\Phi \text{ vertex} \sim \frac{p^2 \alpha_\Phi/3}{p^2 + M_\pi^2} \sim \alpha_\Phi/3. \quad (\text{A2})$$

I include the factors of $1/3$ since, given the definition $\Phi_0 = \text{Str}(\Phi)/\sqrt{3}$, they are generic. Including these results the power counting for \mathcal{L}_0 is

$$\mathcal{A}_N \sim \frac{\chi}{f^{N-2}} (\epsilon^2)^{n_\ell - n_\delta} (\delta)^{n_\delta} \left(\frac{\alpha_\Phi}{3}\right)^{n_\alpha}, \quad (\text{A3})$$

where n_δ and n_α are, respectively, the number of m_0^2 and α_Φ vertices. The appearance of $1/\epsilon^2$ in the contribution of the m_0 vertex in eq. (A2) is the reason for the modification of power counting in quenched chiral perturbation theory. As discussed below, one typically chooses $\delta \geq \epsilon^2$, so that additional m_0^2 vertices either come at “no cost” or are enhanced.

There is, however, a constraint on the number of m_0^2 and α_Φ vertices due to the cancellation of internal quark and ghost loops. A simple example of this constraint is that one cannot have two such vertices on the same propagator, since this would require an internal quark loop. As I will explain, the general form of this constraint is

$$n_\delta + n_\alpha \leq n_\ell + n_{cut}, \quad (\text{A4})$$

where n_{cut} is the number of independent purely gluonic “cuts” through the correlator. In other words, if one traces the quark lines, they will fall into $n_{cut} + 1$ quark-disconnected components. In perturbation theory the only connection between these components is provided by gluons. In the cases of interest here, the connected correlator $\hat{\Delta}_c(p)$ has $n_{cut} = 0$, while the hairpin correlator $\hat{\Delta}_h(p)$ has $n_{cut} = 1$.

⁷ This also holds for the corresponding 1PI correlator, and thus for the N-point scattering amplitude, although I will not use this here.

To demonstrate the result (A4) I first consider correlators with $n_{cut} = 0$, i.e. those which are connected in terms of quark lines. I need the result that the four and higher-point vertices coming from \mathcal{L}_0 involve a single supertrace, and thus are themselves singly connected in terms of quark line diagrams. The cancellation of diagrams with internal quark loops then implies the following: there must be at least one path through the (pion language) diagram from each m_0^2 or α_Φ vertex to each of the external pions which does not pass through another m_0^2 or α_Φ vertex. This must be true if one leaves the original vertex in either direction. Were this not the case, there would be a segment of the diagram completely “cut-off” by m_0^2 and α_Φ vertices, corresponding to an internal quark loop in the quark-line language.

A corollary of this result is that, if one were to “pull apart” each of the m_0^2 and α_Φ vertices to give two extra external pions for each such vertex, then the resulting “expanded” pion-language diagram is singly connected (in the usual sense).

Now imagine starting with an unquenched chiral perturbation theory diagram and adding as many m_0^2 and α_Φ vertices as possible on the propagators. When this has been done, the corresponding expanded diagram must be a tree diagram, since if there were any loops, the internal propagator(s) could be expanded by adding additional m_0^2 or α_Φ vertices. It must also be a singly connected (pion-language) diagram from the corollary of the previous paragraph. Now, when one now sews the m_0^2 and α_Φ vertices back together again, each leads to an independent loop momentum in the original diagram, and thus $n_\delta + n_\alpha = n_\ell$. Since this is the maximum number of such vertices that can be added, one finds the inequality (A4) with $n_{cut} = 0$.

The generalization to $n_{cut} > 0$ is straightforward. One can now have additional m_0^2 and/or α_Φ vertices, since n_{cut} of them can be used to separate the $n_{cut} + 1$ quark-disconnected components of the diagram. Thus one finds the general inequality of eq. (A4).

When using this formula two additional results should be borne in mind. First, there is, in general, no non-trivial lower limit on the number of m_0^2 and α_Φ vertices. One might have expected the constraint $n_\delta + n_\alpha \geq n_{cut}$, i.e. that m_0^2 and α_Φ vertices are necessary to lead to quark-disconnected components. This is not the case, however, because loop diagrams involving connected vertices can lead to quark-disconnected correlators, as discussed in Refs. [14, 18] for the hairpin vertex. Second, even if a given choice of n_δ , n_α and n_ℓ satisfies the constraint in eq. (A4), there may not be a diagram contributing to \mathcal{A}_N . Examples of this will be seen below.

2. Including \mathcal{L}_1 and higher order Lagrangians

It is straightforward to include the “standard” $O(\epsilon^4)$ Lagrangian, \mathcal{L}_{1A} , in the power counting. Each vertex from \mathcal{L}_{1A} gives an additional factor of ϵ^2 , as in the unquenched theory, and the constraint on $n_\delta + n_\alpha$ remains unchanged. It should be borne in mind, however, that since some of the vertices in \mathcal{L}_{1A} contain two supertraces, it becomes more complicated to determine the “quark-line connectivity” of a given graph. This has no impact on the generic power counting, but means that a larger number of diagrams will vanish in the quenched theory.

As noted in the text, one must also consider operators which are built upon those in \mathcal{L}_0 and \mathcal{L}_{1A} by multiplying by additional factors of Φ_0/f . Two examples are given in eq. (3). The key observation is that these factors have the same power of $1/f$ as vertices arising from the expansion of $U = \exp(2i\Phi/f)$. Thus the power counting is unchanged, as long as n_δ and n_α are generalized to be the number of vertices built upon the original m_0^2 and α_Φ vertices, respectively. Thus, for example, n_δ becomes the total number of vertices of the form $(\Phi_0)^q$ with $q = 2, 4, 6, \dots$. What is changed is the connectivity of the diagram. Each extra factor of Φ_0/f requires an additional loop, or gluonic cut, in the diagram, since Φ_0 closes off quark lines. Thus the loop constraint generalizes to $n_\delta + n_\alpha + n_\phi \leq n_\ell + n_{cut}$, where n_ϕ is the total number of extra factors of Φ_0 in the diagram. Note that a $(\Phi_0)^4$ vertex contributes both to n_δ (which it increments by one) and to n_ϕ (which it increments by two).

Each vertex involving extra factors of Φ_0 comes with a new coupling, e.g. $v_{0,8}$ in \mathcal{L}_{1B} . These couplings are suppressed in the large N_c limit because a Φ_0 vertex is connected only by gluons to the rest of the diagram. Each additional Φ_0/f leads to a suppression by $1/N_c$. For example, if the quark loop is connected by two gluons to the rest of the diagram, there is an additional color loop, and the counting is $g^4 N_c = (g^2 N_c)^2 / N_c \sim 1/N_c$. (The $\sqrt{N_c}$ contained in f is exactly that needed to create a state which is correctly normalized in the large N_c limit.) Thus I find that $v_8 \sim 1/N_c$ and $v_0 \sim 1/N_c^2$. For a general diagram, the additional suppression is by $(N_c)^{-n_\phi}$.

I should stress that I am not claiming to extract the full N_c dependence of diagrams. There is also implicit N_c dependence in f , in some of the Gasser-Leutwyler coefficients, L_i , and in m_0^2 and α_Φ . Indeed the latter two are both proportional to $1/N_c$ [1]. My idea is that, based on the general success of the OZI rule, it is likely that constants such as v_8 and v_0 are suppressed relative to unity. Keeping track of the powers of $1/N_c$ associated with these constants allows one to implement this as one deems appropriate.

Higher order terms in the quenched chiral Lagrangian involve more derivatives (acting on either U or Φ_0) and more factors of χ . These can be accounted for, along with those from vertices in \mathcal{L}_{1A} , by introducing the quantity n_1 , which

counts the number of factors of χ plus half the number of derivatives *beyond those that would appear if the vertices were from the lowest order Lagrangian \mathcal{L}_0* . Thus a vertex from the standard chiral Lagrangian with six derivatives and one factor of χ would increment n_1 by three. Overall, diagrams are multiplied by an extra factor of $(\epsilon^2)^{n_1}$.

There is an ambiguity in this definition of n_1 : does, for example, the vertex proportional to $(\partial\Phi_0)^4$ count as $n_\delta = 1$, $n_\phi = 2$ and $n_1 = 2$ or as $n_\alpha = 1$, $n_\phi = 2$ and $n_1 = 1$? In other words, does it contribute a correction proportional to $\delta\epsilon^2/N_c^2$ or to $(\alpha_\Phi/3)\epsilon^4/N_c^2$? These are not the same size in some power counting schemes, e.g. those discussed below. The ambiguity arises because dimensions can be balanced either by powers of m_0 or powers of f . In fact, this ambiguity also arises for the Φ_0^q vertices without derivatives, and I have chosen there the overall factor of m_0^2/f^{q-2} rather than $1/f^{q-4}$. Fortunately, for the calculation considered in the main text, I can leave this ambiguity unresolved, as the operators in question do not contribute until higher order than that I consider.

The preceding considerations together imply the following final power counting result:

$$\mathcal{A}_N \sim \frac{\chi}{f^{N-2}} (\epsilon^2)^{n_\ell - n_\delta + n_1} (\delta)^{n_\delta} \left(\frac{\alpha_\Phi}{3}\right)^{n_\alpha} \left(\frac{1}{N_c}\right)^{n_\phi}, \quad n_\delta + n_\alpha + n_\phi \leq n_\ell + n_{cut}. \quad (\text{A5})$$

3. Applying the power counting

I now apply the result (A5) to the examples considered in the text, namely the two-point quark-connected and disconnected correlators (i.e. \mathcal{A}_2 with $n_{cut} = 0$ and 1 respectively). To do so I must decide how to treat δ , α_Φ and $1/N_c$ relative to each other and to ϵ^2 . This depends, of course, on the size of quark masses considered. I have in mind mesons somewhat lighter than the kaon mass, so that $\epsilon^2 \approx 0.2$.

I consider two possibilities for the relative size of the different terms. The first is

$$\text{PC1:} \quad \delta \sim \frac{\alpha}{3} \sim \frac{1}{N_c^2} \sim \epsilon^2 \quad \Rightarrow \quad \mathcal{A}_N \sim \frac{\chi}{f^{N-2}} (\epsilon^2)^{n_\ell + n_1 + n_\alpha + n_\phi/2}, \quad (\text{A6})$$

which one might call “standard” power counting. The key choices here are that $\delta \sim \epsilon^2$, so that there is no extra enhancement of the m_0^2 vertices, and that $\alpha_\Phi/3$ is small. One might argue that $\alpha_\Phi/3 \sim \epsilon$, rather than ϵ^2 , because it is proportional to $1/N_c$. I prefer the smaller choice given the numerical evidence that $\alpha_\Phi \ll 1$.

The second scheme is

$$\text{PC2:} \quad \delta \sim \frac{\alpha}{3} \sim \frac{1}{N_c^2} \sim \epsilon^{4/3} \quad \mathcal{A}_N \sim \frac{\chi}{f^{N-2}} (\epsilon^2)^{n_\ell + n_1 - n_\delta/3 + 2n_\alpha/3 + n_\phi/3}. \quad (\text{A7})$$

This enhances the contributions from Φ_0 vertices relative to “standard” chiral vertices, and is the power counting used in the text. The power of ϵ is chosen for a reason that will be explained below. In fact, most features of the power counting, including the application discussed in the main text, are unchanged if $\epsilon^{4/3}$ is replaced with ϵ .

Table I collects the contributions to the quark-connected correlator which are of size ϵ^4 or smaller relative to the leading order, in one or both power counting schemes. Table II gives the analogous contributions to the hairpin correlator, though only up to size $\epsilon^{10/3}$. I list all contributions consistent with the constraint in eq. (A5), but, as can be seen from the table, some are absent in quenched chiral perturbation theory. For example, the standard one-loop “tadpole” diagram ($n_\ell = 1$, all other n ’s zero) requires an internal quark loop for $n_{cut} = 0$, although, as observed in Refs. [14, 18], it is present for $n_{cut} = 1$. Another constraint is that the only term with $n_\phi = 1$ and $n_1 = 0$, namely the interaction quoted in eq. (11), can be (and I assume has been) removed by a field redefinition.

To illustrate the difference between the power counting schemes, and the general nature of the chiral expansion in quenched chiral perturbation theory, I discuss the application to the pseudo-Goldstone pion mass. This can be obtained from the amputated quark-connected vertex. In the **PC1** scheme, NLO contributions to the quark-connected correlator are from the Gasser-Leutwyler constants (entering at tree level) and the m_0^2 vertex (at one loop). The result for the pion mass is

$$\frac{M_\pi^2}{\chi} = 1 - \delta[\log(\chi/\mu^2) - 1] + 8(2L_8 - L_5) \frac{\chi}{f^2}, \quad (\text{A8})$$

in dimensional regularization and the renormalization scheme of Ref. [16]. The α_Φ vertex first contributes at NNLO, and is but one of many terms, including three-loop diagrams with three m_0^2 vertices!

The **PC2** scheme is in part an attempt to systematize the power counting scheme used in BDET. This involves keeping corrections of size $\delta\epsilon^2 \log(M_\pi)$, while those of size ϵ^4 are dropped. Here I am not treating $\log(M_\pi/\mu)$ as large, so I must take δ larger than ϵ^2 , which leads to a scheme like **PC2**. The choice $\delta \sim \epsilon^{4/3}$ is made (as opposed to $\delta \sim \epsilon$, say) so that the three loop δ^3 contribution is smaller than the $\delta\epsilon^2$ correction. Nevertheless Table I shows that keeping

TABLE I: Leading contributions to the quark-connected two-point correlator in quenched chiral perturbation theory. **PC** gives the size of the diagram relative to $\mathcal{A}_2 = \chi$ using the general power-counting formula, eq. (A5), while **PC1** and **PC2** refer to the two specific schemes discussed in the text. All contributions up to relative size ϵ^4 in one or both power-counting schemes are included. The references to fig. 3 refer to the parts of the diagrams to the left of the rightmost hairpin vertex (which are thus quark-connected).

n_ℓ	n_δ	n_α	n_1	n_ϕ	PC	PC1	PC2	Figure	Comment
0	0	0	0	0	1	1	1		
0	0	0	1	0	ϵ^2	ϵ^2	ϵ^2	3(b)	L_5 and L_8 contribute
0	0	0	2	0	ϵ^4	ϵ^4	ϵ^4		
1	0	0	0	0	ϵ^2				Absent
1	1	0	0	0	δ	ϵ^2	$\epsilon^{4/3}$	3(a)	Quenched Chiral Log
1	0	0	0	1	ϵ^2/N_c				Absent
1	0	1	0	0	$(\alpha_\Phi/3)\epsilon^2$	ϵ^4	$\epsilon^{10/3}$	3(a)	Leading α_Φ term
1	1	0	1	0	$\delta\epsilon^2$	ϵ^4	$\epsilon^{10/3}$	3(e)	L_3 , L_5 , L_8 , and L_Q contribute
1	0	0	1	0	ϵ^4	ϵ^4	ϵ^4		
2	1	0	0	0	$\delta\epsilon^2$				Absent
2	2	0	0	0	δ^2	ϵ^4	$\epsilon^{8/3}$	3(c,d)	Full result not available
2	0	0	0	0	ϵ^4	ϵ^4	ϵ^4		
2	1	0	0	1	$\delta\epsilon^2/N_c$				Absent
3	3	0	0	0	δ^3	ϵ^6	ϵ^4		

TABLE II: Leading contributions to the hairpin (quark-disconnected) two-point correlator in quenched chiral perturbation theory. All contributions up to $\epsilon^{10/3}$ relative to the leading order term in one or both power-counting schemes are included. Notation as in Table II. The references to figs. 3 and 4 refer to the entire diagram.

n_ℓ	n_δ	n_α	n_1	n_ϕ	PC	PC1	PC2	Figure	Comment
0	0	0	0	0	1				Absent
0	1	0	0	0	δ/ϵ^2	1	$\epsilon^{-2/3}$	4(a)	m_0 vertex
0	0	1	0	0	$(\alpha_\Phi/3)$	ϵ^2	$\epsilon^{4/3}$	4(a)	α_Φ vertex
0	1	0	1	0	δ	ϵ^2	$\epsilon^{4/3}$	3(b)	Wavefunction renormalization from L_5
0	0	0	1	0	ϵ^2	ϵ^2	ϵ^2	4(b)	Two-supertrace vertex from L_7
0	0	0	0	1	$1/N_c^2$				Absent
0	0	0	1	1	ϵ^2/N_c	ϵ^3	$\epsilon^{8/3}$	4(e)	v_8 vertex
1	0	0	0	0	ϵ^2	ϵ^2	ϵ^2	4(c)	Present even in quenched theory
1	1	0	0	0	δ				Absent
1	2	0	0	1	δ^2/ϵ^2	ϵ^2	$\epsilon^{2/3}$	3(a)	No contribution to \mathcal{D} or \mathcal{S}
1	2	0	1	0	δ^2	ϵ^4	$\epsilon^{8/3}$	3(e)	Wavefunction renormalization from L_3 , L_5 and L_Q
1	1	1	0	0	$\delta(\alpha_\Phi/3)$	ϵ^4	$\epsilon^{8/3}$	3(a)	No contribution to \mathcal{D} or \mathcal{S}
1	1	0	0	1	δ/N_c				Absent
2	3	0	0	0	δ^3/ϵ^2	ϵ^4	ϵ^2	3(c,d),4(d)	Full result not yet available
2	2	0	0	0	δ^2	ϵ^4	$\epsilon^{8/3}$		

the $\delta\epsilon^2$ correction, which is of size $\epsilon^{10/3}$, requires keeping many other terms. Most have been calculated, but not all. Those not yet calculated are the non-trivial two-loop diagrams involving two m_0^2 vertices [Fig. 3(d)], and a subset of the contributions of size $\sim \delta\epsilon^2$ from Fig. 3(e). The latter receives contributions not only from the L_5 and L_8 vertices (calculated in BDET) but also from the L_3 and L_Q vertices (not yet calculated).

One can go to higher order in δ if one assumes that $\log(M_\pi/\mu)$ is large, and keeps all terms of size $[\delta \log(M_\pi/\mu)]^n$. This requires calculating only the tadpole loops, the simplest examples being figs. 3(a) and (g), and these can be summed to all orders [2]. This may be required when working at the smallest quark masses used in present quenched

simulations [8, 9, 10].

The results in Table II are used in the calculation in the text, and are discussed further there. I only note here that an important simplification is that fig. 3(a) does not contribute to \mathcal{D} and \mathcal{S} . This would have been the leading correction to \mathcal{D} and the leading term in \mathcal{S} . It does not contribute because the tadpole loops involving the m_0^2 vertex do not give rise to wavefunction renormalization. This follows in turn because the vertex coupling two Φ_0 fields to two non-singlet pions comes only from the mass term $\text{Str}(\chi U) + h.c.$ and not from the derivative term $\text{Str}(\partial U \partial U)$.⁸

-
- [1] C. W. Bernard and M. F. Golterman, Phys. Rev. D **46**, 853 (1992) [arXiv:hep-lat/9204007].
 - [2] S. R. Sharpe, Phys. Rev. D **46**, 3146 (1992) [arXiv:hep-lat/9205020].
 - [3] W. A. Bardeen, A. Duncan, E. Eichten and H. Thacker, Phys. Rev. D **62**, 114505 (2000) [arXiv:hep-lat/0007010].
 - [4] W. Bardeen, E. Eichten and H. Thacker, arXiv:hep-lat/0307023.
 - [5] Y. Kuramashi, M. Fukugita, H. Mino, M. Okawa and A. Ukawa, Phys. Rev. Lett. **72**, 3448 (1994).
 - [6] J. Heitger, R. Sommer and H. Wittig [ALPHA Collaboration], Nucl. Phys. B **588**, 377 (2000) [arXiv:hep-lat/0006026].
 - [7] T. DeGrand and U. M. Heller [MILC collaboration], Phys. Rev. D **65**, 114501 (2002) [arXiv:hep-lat/0202001].
 - [8] S. J. Dong, T. Draper, I. Horvath, F. X. Lee, K. F. Liu, N. Mathur and J. B. Zhang, arXiv:hep-lat/0304005.
 - [9] T. W. Chiu and T. H. Hsieh, arXiv:hep-lat/0305016.
 - [10] C. Gattringer *et al.* [BGR Collaboration], arXiv:hep-lat/0307013.
 - [11] S. R. Sharpe, Nucl. Phys. Proc. Suppl. **53**, 181 (1997) [arXiv:hep-lat/9609029].
 - [12] H. Wittig, arXiv:hep-lat/0210025.
 - [13] S. R. Sharpe and R. S. Van de Water, arXiv:hep-lat/0310012.
 - [14] S. R. Sharpe and N. Shores, Phys. Rev. D **62**, 094503 (2000) [arXiv:hep-lat/0006017].
 - [15] J. Smit and J. C. Vink, Nucl. Phys. B **286**, 485 (1987).
 - [16] J.F. Donoghue, E. Golowich and B.R. Holstein, “*Dynamics of the standard model*,” Cambridge Univ. Pr. (1992).
 - [17] S. R. Sharpe and N. Shores, Phys. Rev. D **64**, 114510 (2001) [arXiv:hep-lat/0108003].
 - [18] S. R. Sharpe, Phys. Rev. D **41**, 3233 (1990).

⁸ This simplification does not hold for the four derivative single supertrace vertices with couplings L_3 and L_Q , which contribute through fig. 3(e), as can be seen in the table.